STATISTICAL ANALYSIS OF MEMBRANE POTENTIAL FLUCTUATIONS

RELATION WITH PRESYNAPTIC SPIKE TRAIN

H. LEVITAN, J. P. SEGUNDO, G. P. MOORE, *and* D. H. PERKEL

From the Departments of Anatomy and Physiology and the Brain Research Institute, University of California, Los Angeles, California 90024, and The RAND Corporation, Santa Monica, California 90406

ABSTRACT In a study of integration at the single neuron level, the relationships between the postsynaptic membrane potential and the presynaptic spike train were analyzed. Fluctuations in membrane potential of neurons in the visceral ganglion of *Aplysia* were measured and described by histograms. The histogram estimates the probability density function of the membrane potential. Comparisons were made among histograms when there was no synaptic input, and when there was a single input in which variations were made in the PSP (postsynaptic potential) sign, i.e. excitatory or inhibitory, and arrival statistics, e.g. slow or fast, regular, Poisson-like, or patterned. This was examined in cells where the membrane potential was constant and in cells in which there was spontaneous pacemaker activity. The form of the histogram depended on whether the neuron was spontaneously quiescent or a pacemaker, or whether it received presynaptic input and, if it did, on the sign and temporal characteristics of such input. From such histograms the mean firing rate of output spike trains can be predicted; additional information of a temporal nature is required, however, to predict features of the interval structure of the output train. Suggestions are made concerning the way the nervous system might utilize the information summarized in the membrane potential histogram.

INTRODUCTION

This work is part of an effort to study integration at the single neuron level by analyzing the relationship between the dynamics of the postsynaptic membrane potential, and the pre- and postsynaptic spike trains. Fluctuations in membrane potential were measured and described by histograms. Comparisons were made among membrane potential histograms when there was no synaptic input and when there was a single input in which variations were made in the PSP sign, i.e. excitatory or inhibitory, and arrival statistics, e.g. slow or fast, regular, Poisson-like or patterned. This was examined in cells where the membrane potential was constant, and in cells where there was spontaneous pacemaker activity.

In general, the following questions may be asked: (*a*) What is the relation between the membrane potential histogram of a postsynaptic neuron and the features of an impinging presynaptic spike train? (*b*) Can one predict the "form" of the output spike train from a neuron given the character of the postsynaptic membrane potential histogram? And (*c*) what suggestions can be made concerning the way in which the nervous system might utilize the information summarized in the membrane potential histogram? Question (*a*) is answered experimentally in the present communication. Questions (*b*) and (*c*) are discussed at a more hypothetical level.

MATERIALS AND METHODS

Experiments were carried out in the isolated visceral ganglion of *Aplysia californica* bathed in natural sea water, at 12–15°C. Five connectives (left and right visceropleural, branchial, genital, and anal) (see Eales, 1921) were each draped over pairs of chlorided silver stimulating electrodes and for optimal preservation, were kept under the water. A small incision was made in the connective tissue enveloping the ganglion, thus exposing small clusters of nerve cells. Intraneuronal recordings were made with glass microelectrodes filled with 2.5 M potassium chloride or 2 M potassium citrate. These were amplified with a Medistor Model A-35 Electrometer preamplifier (Medistor Instrument Co., Seattle, Wash.) and then stored on FM magnetic tape (Sanborn 2000 tape recorder, Sanborn Co., Waltham, Mass.). Once a cell was impaled, a systematic search was made to determine which, if any, of the connectives provided synaptic input upon stimulation. Trains of evenly spaced stimuli or of evenly spaced pairs or trios of stimuli were used. On other occasions, the stimulator was triggered by a Geiger counter exposed to a weak radioactive source, and the mean rate was set by adjusting the position of the source. The 50 msec dead time, or minimum time permitted between consecutive stimuli, was determined by appropriately setting the minimum pulse interval on the waveform generator. Random stimuli from such a source are well-defined statistically (Feller, 1966) and spike trains with these properties have been found to occur naturally in the nervous system (Moore et al., 1966). When it was desired to study only the subthreshold oscillations of the membrane potential undisturbed by action potentials, spiking was prevented by passing a hyperpolarizing current through the recording electrode.

Two classes of neurons were studied. "Quiet" cells had a relatively stable resting potential, received no apparent spontaneous synaptic input, and did not fire spontaneously. "Pure pacemaker" cells fired periodically after a slow drift of the membrane potential to threshold and also lacked obvious spontaneous synaptic input (Junge and Moore, 1966). The records selected for subsequent analysis were taken from sections of data which were judged to be "stationary" by the criterion that the fluctuations in membrane potential were relatively constant under constant experimental conditions. Selection of stationary data segments was performed mostly by eye with some confirmation provided by segmenting long records for separate analysis before pooling.

Our analysis centered upon the values of the membrane potential. The signals on the analogue tape were digitized at rates between 250 and 1000 samples/sec and computation of membrane potential histograms and related quantities (mean, standard deviation) was performed on the console system of an SDS 930 (Scientific Data Systems, Santa Monica, Calif.) digital computer (Betyar, 1967). This kind of analysis affords only a partial description of the phenomenon, ignoring the temporal sequential characteristics. In spite of this, it is revealing to examine the values and limitations of the method.

The *membrane potential histogram*[1] estimates the probability density function of the membrane potential. It is a display of the relative time spent at a particular membrane potential on the ordinate, against the membrane potential on the abscissa. Fig. 1 is illustrative. The

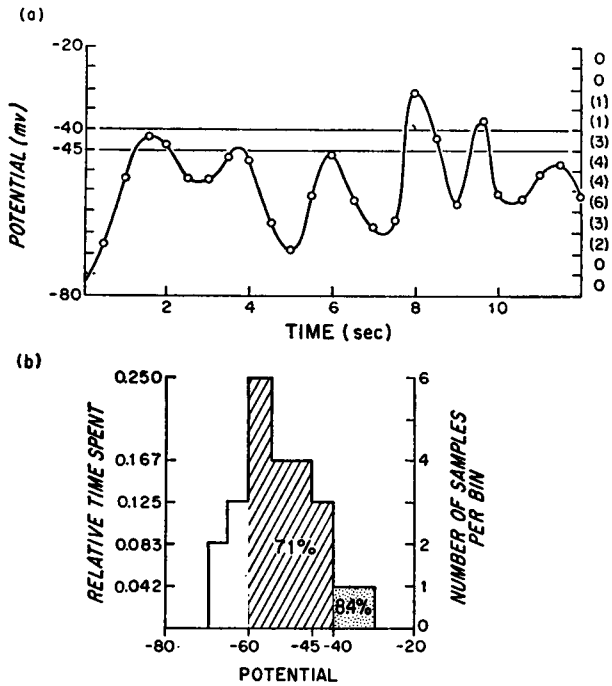

FIGURE 1 Membrane potential histogram for hypothetical voltage fluctuations. (*a*) Hypothetical fluctuations of potential with time. Sampling is at a rate of 2/sec and the extracted voltage values are indicated by open circles. The voltage range from −80 to −20 mv was divided into 5 mv bins. The number of samples in each bin is indicated on the right. (*b*) Histogram of potential in (*a*). Abscissa gives range of potential and is divided into 5 mv bins. Ordinate to right gives number of entries per bin. Ordinate to left gives relative time spent in each bin and is obtained by dividing the number per bin by the total number of samples (24 in this case). The histogram is said to be normalized when the number in each bin is expressed as a fraction of the total number of entries, i.e., when the area under the histogram is 1.

variations in time of a hypothetical potential are drawn in Fig. 1 *a* (solid line). The function is digitized at a rate of 2 samples/sec and the potential values indicated by the open circles are extracted. To obtain the histogram from the digitized values, the voltage scale is partitioned into bins 5 mv wide (left vertical axis) and the number of samples in each bin is counted (numbers at right). For example, in the −40 to −45 mv bin there are three samples. To obtain the membrane potential histogram the number of samples in each bin is plotted against the voltage range (Fig. 1 *b*). Dividing the entry in each bin by the total number of entries, one obtains the relative time spent at each potential. The area under the histogram between any

[1] The distribution function $F(x)$ is given by the integral of the density function,

$$F(x) = \int_{-\infty}^{x} f(y)\, dy$$

two values of potential estimates the fraction of time during which the potential lies between these values, and the area to the right of a particular potential gives the fraction of time the potential is above, i.e. less negative than, that value. In the example in Fig. 1, the potential spends 71% of the time between −60 and −40 mv (cross-hatched area) and 8.4% of the time is less negative than −40 mv (stippled area). The relative area under the histogram to the right of the threshold value estimates the probability that the cell will fire. In the example shown, if the threshold were −40 mv there would be about an 8.4% probability that an output would be observed at any moment in time.

All subsequent histograms have 144 bins on the abscissa with those representing more negative potentials to the left. Histograms are normalized to unity area when the relative

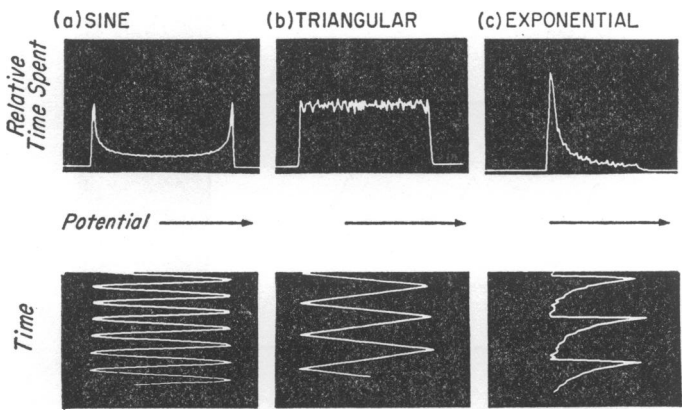

FIGURE 2 Histograms of common periodic functions. Examples of histograms derived from periodic sine (*a*), triangular (*b*), and exponential (*c*) functions, generated electronically and digitized in the same way as the intracellular records. Each display shows a sample of the digitized potential as a function of time, running vertically, and above it the corresponding histogram. (*a*) The sinusoid spends relatively more time at the extreme values than between peaks, so the histogram shows a mode at each extreme of the range. (*b*) The triangular function is linear between the extremes and spends an equal amount of time at all potentials, thus yielding a uniform histogram. (*c*) The step function with exponential decay has a histogram with a mode corresponding to the level of potential which the function approaches exponentially. The histograms in this and subsequent illustrations were taken from the display scope of the digital computer which calculated the histograms. The scope display connects the maxima of each bin with a line.

times spent over a particular potential range are to be compared. They are scaled to equal modal heights when the emphasis is on their shapes.

The probability density functions for periodic sine, triangular, and exponential functions are plotted as illustrative examples in Fig. 2 and derived mathematically in the Appendix.

RESULTS

The experimental results are concerned mainly with the relation between the membrane potential histogram of the postsynaptic neuron and the features of the impinging presynaptic spike train. We first consider the histograms produced by excitatory input of regular, irregular, and patterned timing as a function of mean

rate. Next, we consider the effects of inhibitory input under similar conditions. Finally, the histograms of pacemaker activity with and without synaptic input are examined.

Membrane Potential Histogram of Quiescent Nerve Cells with EPSP's

A single regular excitatory input to a neuron lacking inherent activity produced the membrane potential fluctuations illustrated in Fig. 3. The rate of arriving excitatory postsynaptic potentials (EPSP's) increases from top to bottom in the

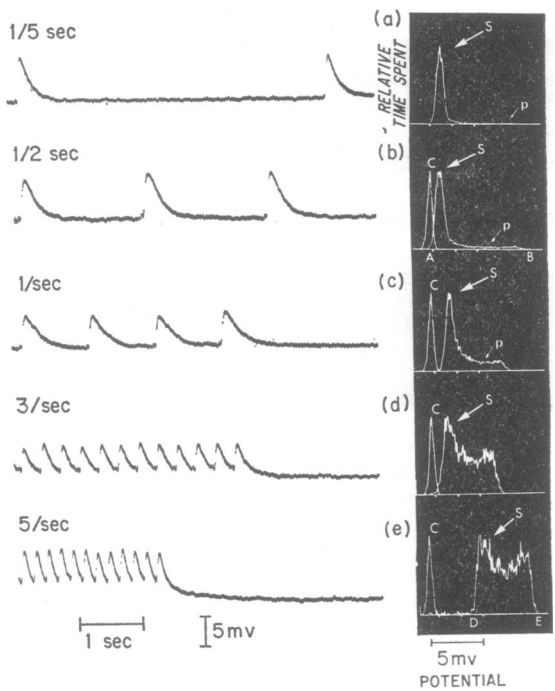

FIGURE 3 Effect of regular excitatory input. At left are intracellular recordings showing EPSP's evoked by stimulation of the right visceropleural connective at different rates. At right and indicated by arrows labeled *S* are the corresponding membrane potential histograms. *p* indicates the plateau in these histograms. The histogram indicated by *C* (shown in all but *a*), represents the membrane potential at rest when no stimuli are delivered. As the EPSP rate increases, from top to bottom, the "stimulated" histogram is displaced more and more to the right, i.e. to more depolarized levels, and its shape changes from positively skewed to more uniform and narrow (compare ranges *AB* in *b* and *DE* in *e*). The mean displacement of the membrane potential from the mean resting level was 1, 2.5, 2.7, 3, and 6.5 mv. The standard deviations were 1.5, 2, 1.7, 1.5, and 2 mv in *a–e*, respectively. The standard deviation of the resting membrane potential was 0.2 mv. Histograms are displayed scaled to equal amplitude. When normalized the modal values are 0.18 for quiescent histogram, *C*, and 0.11, 0.07, 0.06, 0.03, and 0.02 for "stimulated" histograms *a-e*, respectively. In all figures, records were taken from tape recordings and histograms were photographed from the CRT (cathode-ray tube) display of the computer.

illustration. After the stimulus stops the membrane potential returns to the resting level. To the right are the corresponding membrane potential histograms scaled to the same maximum height. In all but the top display, there are two superimposed histograms. The narrow one to the left (labeled *C*) represents the membrane potential at rest, before or after a train of PSP's. Its narrowness indicates that there is little deviation from the mean resting level. To the right of this histogram, toward more depolarized levels, is the membrane potential histogram during the stimulus train (*S*). As the EPSP arrival rate increases, the "stimulated" histogram is displaced more and more to the right. Its shape also changes from skewed to more narrow and uniform. At low arrival rates (1/5, 1/2, and 1 per sec), the histograms are positively skewed, with the mode more negative than the mean, because a greater proportion of the time is spent near the resting level. At more depolarized levels, these histograms show a plateau (*p*) indicating that the PSP spends a relatively uniform amount of time at these potentials. This uniformity is due to the approximately linear rise and fall in the EPSP near its peak. At higher arrival rates, the "stimulated" histograms become narrowed because the size of the oscillation is reduced (compare *A-B* in *b* with *D-E* in *e*). The amplitude is reduced partly because the membrane potential does not have sufficient time to return to the resting level before the next PSP arrival and partly because the amplitude of the PSP initiated from more depolarized levels is decreased. The histograms are more uniform at these high rates because relatively more time is spent along the quasi-linear portion of the EPSP's.

Fig. 4 *a* compares the potential fluctuations under regular and Geiger-driven stimulations at a mean rate of 3/sec. The mean depolarization from the resting level is 10.7 mv for both cases, but the standard deviations are markedly different being 2 and 4.5 mv for regular and Geiger stimulation, respectively. Each input form produces a different membrane potential histogram. A narrow, relatively uniform histogram was derived from the regular synaptic activation, but a broad skewed histogram was produced by Geiger-driven excitation. The curves have been normalized to unity area. The histograms show that the two inputs will not be equally effective in evoking discharge from the cell. For a spike threshold, like *A* in the figure, that is relatively high and less negative than the mean depolarization level, the Geiger-driven stimulus would be more effective, because the corresponding histogram indicates that the potential spends a greater fraction of time above threshold. Contrastingly, with a threshold like *B*, more negative than the mean depolarization level, the regular stimulation would be more effective. This difference in effectiveness of two inputs is illustrated in Fig. 4 *b*, where the threshold for spike discharge is less negative than the mean depolarization level. Regular EPSP input yields no spike output, while Geiger-driven input of the same mean rate produced several spikes.

Comparison of the histograms produced by regular and Geiger-driven stimulation at several rates is made in Fig. 5. As the mean rate of stimulation increases from 1 to 3/sec, both sets of "stimulated" histograms (labeled *S*) tend to present higher

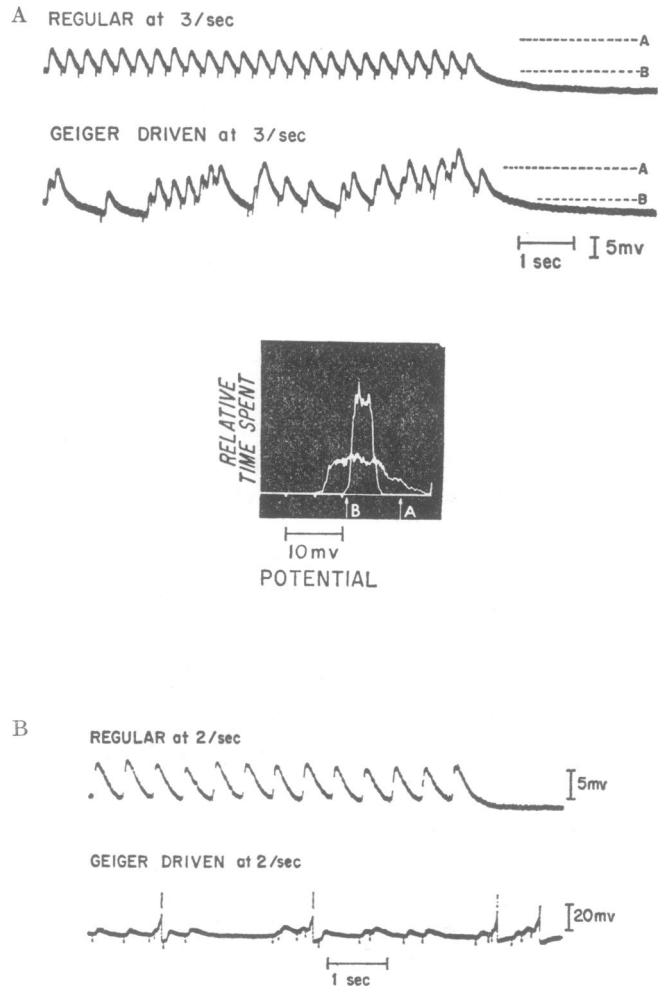

FIGURE 4 Comparison of effect of regular and irregular EPSP's. (*A*) Membrane potential fluctuations of cell receiving a single excitatory input at a mean rate of 3/sec, regularly (top) and irregularly (bottom). The mean displacement of the membrane potential from its resting level was 10.7 mv under both types of stimulation. The standard deviation about the mean was 2 mv for regular stimulation and 4.5 mv for the irregular (Geiger-driven) stimulation. Below are the histograms associated with these oscillations. The relatively narrow and uniform histogram corresponds to regular excitations, the broad and skewed histogram is the result of Geiger-driven excitation. Normalized histograms have modal values of 0.06 and 0.02 for regular and Geiger-driven cases, respectively. Values of potential indicated by *A* and *B* in the intracellular records correspond approximately to the levels of potential so labeled in the histogram. (*B*) Comparison of the effectiveness of Geiger-driven and regular excitatory input in initiating a spike output. No spikes are evoked by regular excitation at 2/sec, but several spikes are evoked by Geiger-driven stimulation at the same mean rate. Gain of lower record is less than that of the upper so that the full extent of the spike could be shown. The size of a single EPSP is the same in both records.

values to the right, i.e., at the less negative potentials. At low rates (upper row) the histograms produced by regular and Geiger-driven stimulation are both heavily skewed with the mode more negative than the mean. This is because at low rates, the membrane potential spends the greatest fraction of time at or near the resting level. The Geiger-driven histograms are distinct in that they lack the plateau present in the "regular" histograms (*p* in Fig. 5) and they extend over a wider range of potential.

Both these differences reflect the extent of temporal summation. With regular stimulation temporal summation is consistent, with each PSP starting from approximately the same level and attaining approximately the same peak amplitude. The linear portion of every PSP occurs over approximately the same range of potentials, and a plateau appears in the membrane potential histogram. With Geiger-driven stimulation the interval between PSP's is irregular, so succeeding

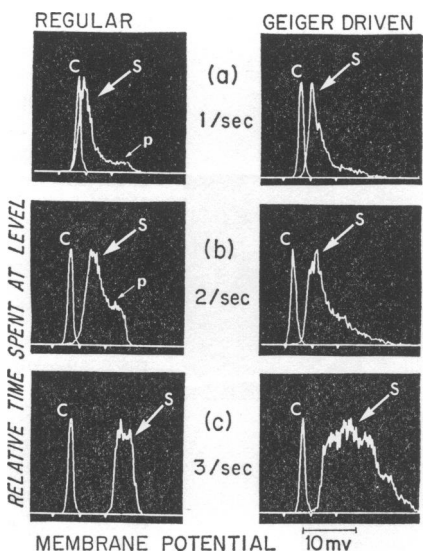

FIGURE 5 Histograms produced by regular and irregular EPSP's of different rates. Comparison of membrane potential histograms produced by regular and Geiger-driven excitatory input as the mean rate of stimulation is increased from 1 to 3/sec. Two histograms are superimposed in each display: the narrow, symmetrical histogram (labeled *C*) represents the control membrane potential at rest, just before or some time after the stimulus train. "Stimulated" histograms are denoted by *S*. *p* indicates plateau in histogram. All histograms are shown scaled to equal modal heights. When normalized the modal values of regularly and Geiger-driven histograms are approximately equal, at 0.07 and 0.04 in *a* and *b*, respectively. In *c* the modal value is 0.06 in the regularly-driven, 0.02 in the Geiger-driven, and 0.22 in the control histograms. Under regular stimulation the mean depolarization of the membrane potential from the resting level is 3, 6, and 10.7 mv and the standard deviation of the membrane potential is 3, 2.7, and 2 mv in *a*, *b*, and *c*, respectively. With Geiger-driven stimulation the mean depolarization is 6, 7, and 10.7 mv and the standard deviation 3.5, 4, and 4.5 mv in *a*, *b*, and *c*, respectively.

PSP's start from different levels and attain different peak amplitudes. The absence of the plateau is then due to lack of coincidence in the linear portions of consecutive PSP's. The irregularity of arriving PSP's also accounts for the greater fluctuations in membrane potential under Geiger-driven stimulation. The membrane potential is deflected to more depolarized levels when driven by closely-spaced EPSP's and drops to potentials close to the resting level when succeeding PSP's are separated

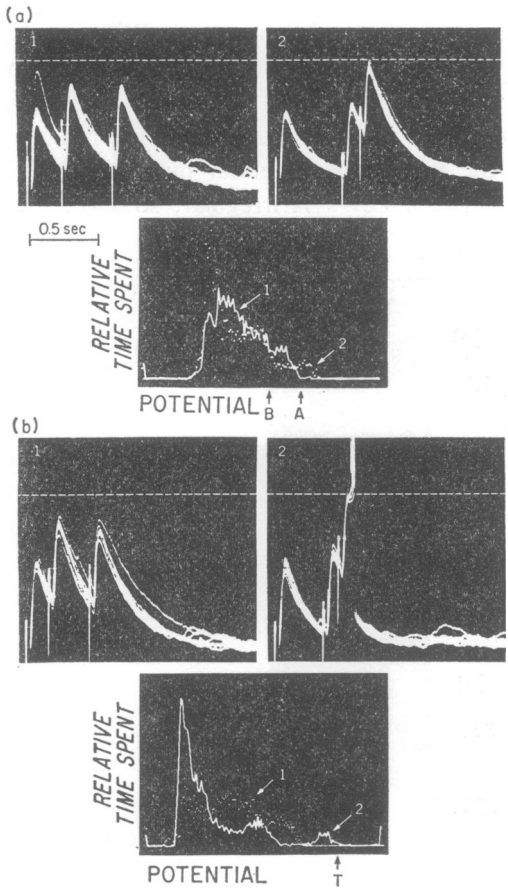

FIGURE 6 Histograms of excitatory trios of varying timing. (*a*) The top row displays, in each frame, twelve superimposed EPSP trios with a span of 575 msec, and with either 250 msec (1, left) or 435 msec (2, right) between the first and second stimuli. The dashed horizontal lines may be used to compare the relative depolarization attained by each pattern. The normalized membrane potential histograms associated with each trio are superimposed below. Histograms 1 (continuous white line) and 2 (dotted line) were produced by trios 1 and 2, respectively, and have modal values of 0.05 and 0.03. (*b*) The top row displays, in each frame, seven superimposed trios with a span of 420 msec, and with either 220 msec (1, left) or 315 msec (2, right) between the first and second stimuli. Trio 2 produces a spike each time. The normalized histograms are superimposed below with the dotted histogram 1 corresponding to trio 1. Modal values are 0.06 and 0.02. *T* indicates the threshold for spike initiation.

by longer intervals. The differences between the histograms produced by regular and Geiger-driven stimulation thus become more marked as the mean PSP rate increases. Under regular stimulation the histogram becomes narrow and more uniform, but that produced under Geiger-driven stimulation becomes broad and retains some skewness (Fig. 5). The mean and the standard deviation of the membrane potential with Poisson arrivals, and with stepwise and constant size PSP's have been calculated (Feller 1966, pp. 175–176).

Segundo, Perkel, and Moore (1968) showed that both the mean rate and pattern

of arriving PSP's were important in determining whether an output spike was evoked from a postsynaptic cell. The variation in the membrane potential histogram of a postsynaptic cell caused by changing the pattern of a stimulus trio is illustrated in Fig. 6. The "long-short" pattern (*2* (arrow), dotted histogram) caused the membrane potential to attain more depolarized levels than the "short-long" pattern (*1* (arrow), continuous histogram) (Fig. 6 *a*). If the spike threshold were at the level indicated by arrow *A*, the "long-short" trio would be more effective in producing an output since this area to the right of the arrow under histogram 2 is greater than that under histogram 1. If, however, the threshold were at *B*, both trios would be equally effective since the areas are approximately equal. When the span of the trio is reduced (Fig. 6 *b*), the membrane potential of the postsynaptic cell reaches threshold *T* after each "long-short" sequence and produces an impulse. A "short-long" stimulus pattern never attains threshold.

Membrane Potential Histogram of Cells with IPSP's

The membrane potential fluctuations produced by single inhibitory postsynaptic potential (IPSP) inputs are described in some cases by histograms which are sym-

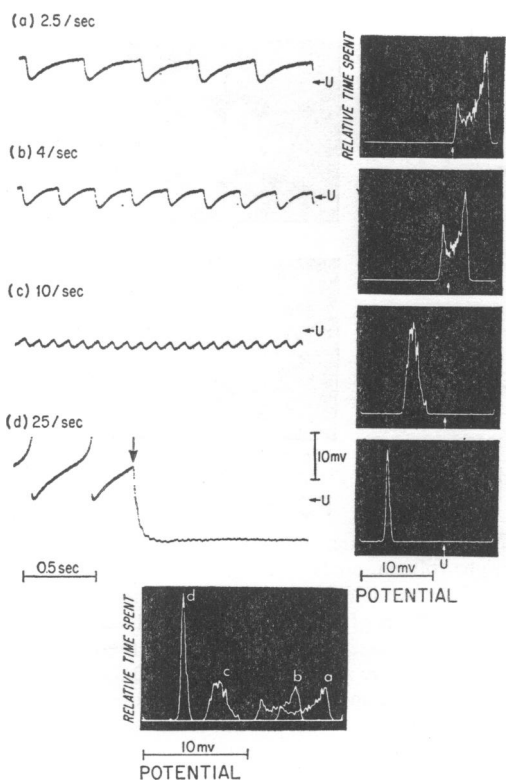

FIGURE 7 Effect of regular inhibitory input. At left, intracellular recordings from cell receiving single inhibitory input at different rates. In the absence of inhibitory stimulation the cell discharged spontaneously. The level of the undershoot that follows each pacemaker spike is indicated by arrow labeled *U* in each record as a reference for comparison of the degree of the hyperpolarization induced by the IPSP's. In *d*, two pacemaker spikes are shown before the initiation (at the arrow) of the evoked IPSP train. The right column shows the corresponding membrane potential histograms. As the stimulus rate increases, from top to bottom, the histograms are shifted to the left, to more negative potentials, and the shape changes from skewed and bimodal to progressively more uniform and finally quite narrow and unimodal. These histograms are scaled to equal modal heights. The four histograms are normalized and superimposed below, where the modal values for histograms *a–d* are 0.06, 0.07, 0.08, and 0.25, respectively.

metric about a vertical axis with those produced by single EPSP input (Fig. 7). For example, at low arrival rates the histograms are skewed with the mode to right of the mean for inhibition and to the left for excitation. As the rate increases the histograms under regular input become bimodal with the predominant mode to the right for inhibition and to the left for excitation. Compare histograms of excitatory input at 3/sec in Fig. 3, with inhibitory input at 2.5/sec in Fig. 7. Irregular stimula-

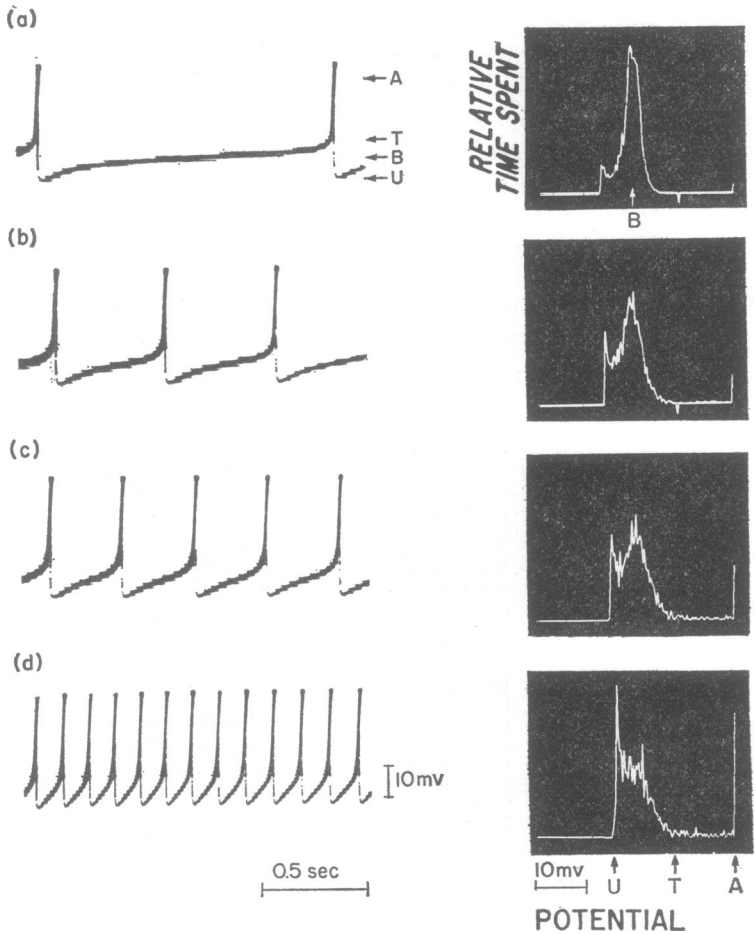

FIGURE 8 Histograms of pacemaker activity. In left column, recording of the same pacemaker cell discharging at various rates. In right column, corresponding normalized membrane potential histograms. The range of the histogram is from the spike undershoot *U* to the potential indicated by level *A* in record. All samples of the spike above this level were entered in the bin at right. As the rate of discharge increases from top to bottom the histograms become more uniform. Normalized histograms have modal values of 0.07, 0.05, 0.05, and 0.07 in *a–d*, respectively. The threshold level *T*, spike undershoot *U*, and the potential *A* indicated in the intracellular records correspond to the levels of potential so labeled in the histograms. The slow pacemaker in *a* spends most of the time at potential *B*, which corresponds to the mode in the associated histogram.

tion produces skewed histograms with the mode to right and left of the mean for inhibitory and excitatory input, respectively. Quite frequently, however, quiescent cells have resting levels which are near to the equilibrium potential for the IPSP and this limits the hyperpolarizing effect of IPSP's at high rates. As a consequence

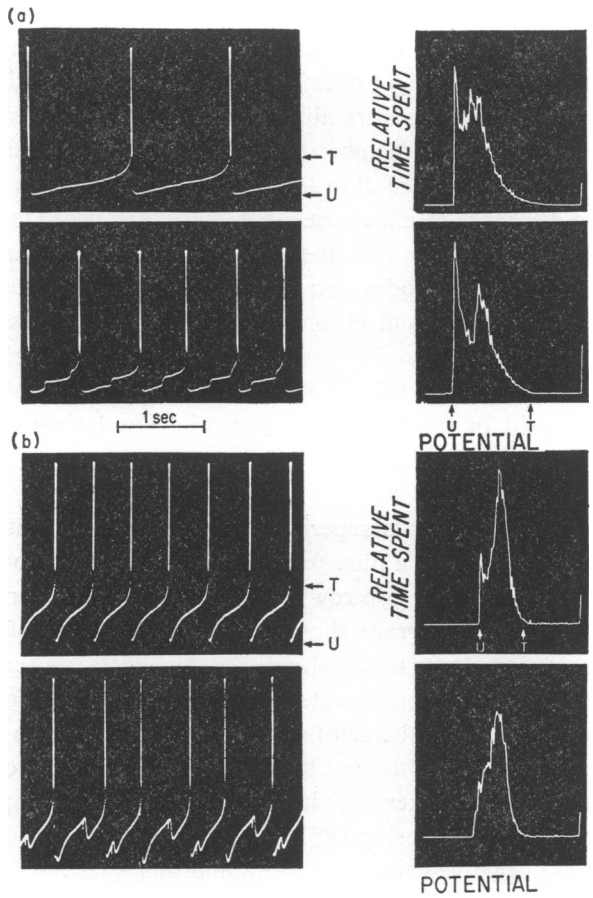

FIGURE 9 Pacemakers with PSP input. (*a*) Left, record of pacemaker with no apparent PSP's (top) and with EPSP's (bottom). The corresponding normalized histograms are shown at right and have approximately equal modal values of 0.04. The addition of EPSP's causes the larger mode to be shifted to the right indicating that the membrane potential spends relatively more time at depolarized levels. The number of entries in the right most bin is greater in the bottom histogram, reflecting the acceleration produced by the EPSP's. (*b*) Left, records from another pacemaker with no apparent PSP's (top) and with regular IPSP input (bottom). The corresponding normalized histograms at right show the shift in the membrane potential to more negative levels when IPSP input is added. Modal values approximately equal at 0.05. The number of entries in the right most bin is smaller in the bottom histogram reflecting the deceleration produced by the IPSP's. Variation in the intensity of the records is due to use of beam brightener circuit.

of this "bottoming" effect the histogram becomes narrow and uniform close to the equilibrium level.

Membrane Potential Histogram of Pacemakers With and Without PSP's

Fig. 8 shows the membrane potential histograms of a pacemaker cell firing at different rates. The range of each histogram extends from the spike undershoot (U) to a potential (A) above threshold. Potential values above level A are entered in the right-hand overflow bin. The height of this bin is therefore proportional to the pacemaker's discharge rate in these normalized histograms. At the slowest discharge rate (top) the pacemaker spends most time between the undershoot U, and the threshold T; the potential labeled B in the record corresponds to the mode in the histogram. As the discharge rate increases (Fig. 8*a–d*) the drift from undershoot to threshold becomes more linear and the corresponding histograms appear more uniform. The more negative modes correspond to the undershoot. They are relatively narrow and show a sharp cut-off on the negative side. The less negative modes correspond to the asymptotic level approached by the pacemaker potential (Junge and Moore, 1966). The gradual fall off of this mode towards threshold is indicative of the exponential drift of the pacemaker potential just before it blends into the spike and may be due to a local potential triggered by an axon spike some distance away (Tauc, 1962).

When a single synaptic input is superimposed upon the pacemaker activity, the histogram is altered. In Fig. 9 *a* a pure pacemaker record is shown together with its membrane potential histogram (top row). When EPSP's are superimposed (second row), the corresponding histogram shows a wider separation of the modes; the right-hand mode shifting closer to threshold, T. This illustrates that the superposition of EPSP's caused the membrane potential to spend a greater fraction of time at more depolarized levels. Since the cell fires more frequently there is an increase in the number of entries in the right-hand bin. In Fig. 9 *b* the effect of superimposing IPSP's is shown. The pacemaker activity is displayed at the top with its corresponding histogram. Superimposing IPSP's causes the potential to spend a greater relative time at more negative values (bottom), and this is reflected in the histogram by a shift to the left and merging of the two modes. The decreased firing rate of the inhibited pacemaker is reflected in a decrease in the number of entries in the right-hand bin.

DISCUSSION

An important function of every neuron, and one related to the transfer of information in the nervous system, is that of maintaining a relation between its presynaptic input and its own postsynaptic discharge. The set of processes determining this input-output relation is defined as integration by Bullock and Horridge (1965). At the single neuron level, integration is determined by the interaction of converging

presynaptic inputs and of the intrinsic properties of the cell, such as its resting potential and threshold. Important issues in integration are therefore reflected by the membrane potential.

Many investigators have attempted to characterize the membrane potential fluctuations produced by natural stimuli and those occurring "spontaneously." The work has been carried out in vertebrate and invertebrate systems ranging from receptor cells (Adolph, 1964), peripheral nerve axons (Derksen and Verveen, 1966; Verveen et al., 1967), and the motor end-plate (Fatt and Katz, 1952) to central elements such as cortical and spinal cord motor neurons (Brock et al., 1952; Katz and Miledi, 1963; Burke and Nelson, 1966; Granit et al., 1966; Hill et al., 1966; Elul, 1967 *a*, *b*). These studies have focused essentially on: (*a*) the source of the fluctuations, and (*b*) the influence of the fluctuation on the excitability and the discharge patterns. Description of membrane potential fluctuations have involved visual examination of the records (Brock et al., 1952; Granit et al., 1966), peak amplitude histograms of PSP-like events (Fatt and Katz, 1952; Adolph, 1964; Burke and Nelson, 1966), calculation of membrane potential, mean and standard deviation (Verveen et al., 1967), membrane potential histograms (Adolph, 1964; Elul, 1967 *a*, *b*), and frequency spectrum analysis (Derksen, 1965; Verveen and Derksen, 1965; Derksen and Verveen, 1966; Hill et al., 1966; Elul, 1967 *b*).

The three questions posed in the introduction concerning the relation between the membrane potential fluctuations of a neuron and its input and output reflect the broad interests of those studying membrane potential fluctuations and our own interest in neuronal integration. In the following paragraphs we show the extent to which the membrane potential histograms afford an answer to these questions. It should be recognized that such histograms render only a partial description since events characterized by certain fluctuations in consistent sequence are ignored.

Our experimental results enable us to answer, to a certain extent, the question of the relation between the membrane potential histogram of a postsynaptic neuron and the features of an impinging presynaptic spike train. The form of the membrane potential histogram depended on whether the neuron was spontaneously quiescent or a pacemaker, on whether or not it received presynaptic input, and, if it did, on the sign (excitatory or inhibitory) and temporal characteristics (i.e., rate and pattern) of the latter.

In summary, (*a*) a *narrow histogram* indicates either a quiescent cell or one receiving very high-frequency synaptic input; the sign of the latter is indeterminate unless the resting level is known. A broader, somewhat skewed histogram is indicative of irregular high-frequency weak synaptic input, and a narrower, more symmetric histogram indicates more regular input. In the limit, with very weak and extremely high-frequency input, regular arrivals may be indistinguishable from irregular arrivals (Segundo, Perkel, Wyman, Hegstad, and Moore, 1968). (*b*) A *bimodal histogram* indicates either pacemaker activity or regular synaptic input of moderate rate; the modes are of unequal width in the former case. In the latter, the

input sign is revealed by the relative position of the dominant mode; it is to the left for excitatory input and to the right for inhibitory. (*c*) Acutely *skewed histograms* are indicative of low input rates, with input statistics indeterminate. The sign of the skew reveals the input sign. Irregular input of moderate to high rate is characterized by broadness, the sign of the skew again revealing the input sign.

We now turn to the question of the way in which the nervous system might utilize the information summarized in the membrane potential histogram, or, in other words, the manner in which the variable "membrane potential histogram" may play a functionally significant role in the normal operation of the nervous system (Moore, 1965). On a purely conjectural basis, it is possible to suggest that the nervous system can estimate the membrane potential histogram of a given cell C by way of the superposition of a "test" excitatory input to the cell under consideration. If each "test" EPSP of amplitude h is sufficiently isolated from other such test events, the probability P that it will bring the membrane potential to threshold T and elicit a spike is the probability that the membrane potential is less negative than T-h when the "test" EPSP arrives. This probability P is $1\text{-}F(T\text{-}h)$, approximated by the area under the histogram and to the right of T-h. P can be estimated by the proportion of times the "test" EPSP's elicits a spike in C in many presentations or by the proportion of cells that fire in a set of cells similar to C in one presentation. By varying the size of the test EPSP and noting the corresponding variation in spike probability, $1\text{-}F(T\text{-}h)$ can be estimated at several values of h, and this in turn provides an approximation to the entire membrane potential probability density. Since the membrane probability density reflects the character of a cell's input (see above), certain knowledge about the latter can be inferred from a determination of the probability of a spike response to test input and does not require explicit intracellular examination.

Finally, we consider the extent to which one can predict the nature of the output spike train from a neuron, given the character of the fluctuations of the membrane potential and of the threshold. This problem has been considered by several investigators. Some have actually recorded the membrane potential fluctuations and attempted a correlation with observed variabilities in spike timing (Derksen, 1965; Verveen and Derksen, 1965; Junge and Moore, 1966; Calvin and Stevens, 1967). Others have attempted a theoretical representation of spontaneous and evoked potential fluctuations, and from such descriptions and a specified threshold behavior, predicted the character of the output spike train (Gerstein and Mandelbrot, 1964; TenHoopen and Verveen, 1963; Stein, 1965; Gluss, 1967). On the basis of our own work, it is evident that only the mean firing rate of the output spike trains can be estimated from membrane potential histograms alone, and that no information can be obtained concerning higher order statistics. The area under a histogram and to the right of the threshold is proportional to the mean discharge rate; the constant of proportionality is given by the duration of the spike wave form at threshold level.

An analysis which included a representation of the frequency power spectrum

or the autocorrelation function of the membrane potential fluctuations (Derksen, 1965; Stein, 1967) would not significantly ameliorate this situation. If the membrane potential is regarded as performing a random walk (e.g. Gerstein and Mandelbrot, 1964) then the interspike-interval histogram may be identified as the histogram of first-passage times (Segundo, Perkel, and Moore, 1968). The problem of determining first-passage times is complicated by the possibility that the initial value, i.e. the undershoot value, may be variable, and the possibility of a moving barrier, i.e., of a time-dependent threshold. A theoretical random-walk formulation of the membrane potential variations embodying sufficient variables so as to reflect realistically the living cases presented above, and implying an explicit solution to the first-passage time problem has not yet appeared. Such a formulation would have to incorporate the following features: (*a*) a choice of arrival statistics, e.g. Poisson arrivals, regular arrivals, etc.; (*b*) a nonlinear summation of PSP's resulting either from the dependence of the PSP amplitude on the extant membrane potential value or from interaction between successive PSP's; (*c*) a shaped recovery of membrane potential after a PSP (e.g. an exponential decay to resting level); and (*d*) the possibility of an over-all drift in membrane potential representing a pacemaker potential.

An empirical approach is possible which preserves temporal information regarding the sequential characteristics of the membrane potential oscillation. One can, for example, estimate the "transition" probabilities $P_t(x, I)$ that the potential will be in the range I at times $t + \tau$ given that it has value x at time t, where t is any time within the observation epoch, or alternately one can define and estimate from intracellular recordings, a family of membrane potential histograms where the parameter τ corresponds to the time after a spike. From the set of such time-dependent membrane potential histograms, the postsynaptic spike autocorrelation can readily be recovered; it is proportional to the area to the right of threshold in the membrane potential histogram at the corresponding time after a postsynaptic spike. Experimental results of this sort will be reported elsewhere. From the estimated autocorrelation it is possible in principle to estimate the interspike-interval histogram, assuming that successive interval lengths are independent, since the two functions are related (Perkel et al., 1967), although this may be difficult in practice. However, even this approach will reveal nothing about the "higher-order" properties of the postsynaptic spike train, such as serial dependencies of interval lengths. For these one needs an even more detailed analysis of the observed dynamics of membrane potential fluctuations.

APPENDIX

Probability Density Functions of Sine, Triangular, and Exponential Functions

To find the probability density function $f(y)$ of the function

$$y = g(t)$$

we solve this equation for all its real roots $t_1, t_2, \cdots t_n$ within the interval of interest $T_1 < t < T_2$. Then

$$f(y) = f(t_1)/|g'(t_1)| + \cdots + f(t_n)/|g'(t_n)|$$

where $f(t)$ is the probability density function of the variable t and $g'(t)$ is the first derivative in time of the function $y = g(t)$. (For proof see Papoulis, 1965, p. 126.)

(*a*) For a sine function where $y = g(t) = A \sin(t + \theta)$, for $A > 0$ over the interval $(-n\pi\ n\pi)$, there are several roots of the form:

$$t_n = \arcsin(y/A) - \theta \quad n = \cdots, -1, 0, 1, \cdots.$$

Since

$$g'(t_n) = A \cos[\arcsin(y/A)] = A[1 - y^2/A^2]^{\frac{1}{2}} = [A^2 - y^2]^{\frac{1}{2}}$$

it follows that

$$f(y) = 1/[A^2 - y^2]^{1/2} \cdot \sum_{-n}^{n} f(t_n) \qquad |y| < A.$$

$[y] > A$, $y = A \sin(t + \theta)$ has no real solutions and thus

$$f(y) = 0 \qquad |y| > A.$$

With t uniformly distributed over the interval $(-n\pi, n\pi)$ the probability density function for t is

$$f(t) = 1/(2n\pi) \quad \text{for} \quad |t| \leqq n\pi$$

$$f(t) = 0 \qquad \text{for} \quad |t| > n\pi.$$

Then

$$f(y) = 1/[A^2 - y^2]^{1/2} \cdot (1/(2n\pi) + 1/(2n\pi) + \cdots) = 2n/(2n\pi[A^2 - y^2]^{\frac{1}{2}})$$

$$f(y) = 1/\pi[A^2 - y^2]^{\frac{1}{2}}$$

which has the shape of the histogram shown in Fig. 2 *a*.

(*b*) For a triangular wave where

$$y = g(t) = -2At/\pi + A \qquad 0 \leqq t \leqq \pi$$

$$= 2At/\pi + A \qquad -\pi \leqq t \leqq 0$$

the roots are $t_1 = -\pi(y - A)/2A$, $t_2 = \pi(y - A)/2A$ in the interval $(-\pi, \pi)$.

Since t is uniformly distributed in the interval $(-\pi, \pi)$

with

$$f(t) = 1/(2\pi) \qquad |t| \leqq \pi$$

$$f(t) = 0 \qquad |t| > \pi$$

and

$$|g'(t_n)| = 2A/\pi$$

the probability density function for y is

$$f(y) = [1/(2\pi)]/[2A/\pi] + [1/(2\pi)]/[2A/\pi]$$

$$= 1/(2A) \quad |y| \leqq A$$

$$f(y) = 0 \qquad |y| > A$$

which is uniform over the values assumed by $g(t)$ and zero elsewhere as in Fig. 2 *b*.

(*c*) For a step function which decays exponentially with time constant τ,

$$y = g(t) = A \exp(-t/\tau) \qquad 0 < t < T$$

$$= 0 \qquad t < 0$$

and there is one root

$$t_1 = -\tau \ln (y/A)$$

in the interval $(0, T)$.
With t uniformly distributed

$$f(t) = 1/T \qquad 0 < t < T$$

$$f(t) = 0 \qquad t < 0$$

and

$$g'(t_1) = (-A/\tau) \exp(-t_1/\tau)$$

$$= (-A/\tau) \exp\{(-1/\tau)[-\tau \ln (y/A)]\}$$

$$= (-A/\tau)(y/A)$$

$$= -y/\tau.$$

Then the probability density function is

$$f(y) = (1/T)/(y/\tau) = (\tau/T)(1/y) \qquad 0 < y < A$$

and

$$f(y) = 0 \qquad y > A, \quad y < 0$$

which is a rectangular hyperbola as shown in Fig. 2 *c*.

When steps of constant height A occur according to a Poisson process of mean rate α, and the time constant is τ, the mean and standard deviation of the membrane values are $\mu = A \alpha \tau$ and $\sigma = A[\alpha\tau/Z]^{\frac{1}{2}}$, respectively (Feller, 1966).

Supported by the National Institutes of Health through a Research Career Program Grant (to J.P.S.) and grants NB-30686; NB-02501; NB-05264; NB-07325 and by Air Force Project RAND. Computing assistance was obtained from the Brain Research Institute's Data Processing Laboratory.

Received for publication 27 April 1968 and in revised form 11 June 1968.

REFERENCES

ADOLPH, A. R. 1964. *J. Gen. Physiol.* **48**:297.

BETYAR, L. 1967. *J. Assoc. Comp. Mach.* **10**:413.

BROCK, L. G., J. S. COOMBS, and J. C. ECCLES. 1952. *J. Physiol. (London).* **117**:431.

BULLOCK, T. H., and G. A. HORRIDGE. 1965. Structure and Function in the Nervous System of Invertebrates. W. H. Freeman & Co., San Francisco, Calif. Chapter 5.

BURKE, R. E., and P. G. NELSON. 1966. *Science.* **151**:1088.

CALVIN, W. H., and C. F. STEVENS. 1967. *Science.* **155**:842.

DERKSEN, H. E. 1965. *Acta Physiol. Pharmacol. Neerl.* **13**:373.

DERKSEN, H. E., and A. A. VERVEEN. 1966. *Science.* **151**:1388.

EALES, N. B. 1921. *Aplysia. Liverpool Mar. Biol. Comm. Mem.* Liverpool University Press, Liverpool, England. 47.

ELUL, R. 1967*a*. *In* Progress in Biomedical Engineering. L. J. Fogel and F. W. George, editors. Spartan Books Inc., Washington, D. C. 131.

ELUL, R. 1967*b*. *In* Proceedings of the 1966 Rochester Conference on Data Acquisition and Processing in Biology and Medicine. Pergamon Press Inc., New York. In press.

FATT, P., and B. KATZ. 1952. *J. Physiol. (London).* **117**:109.

FELLER, W. 1966. An Introduction to Probability Theory and Its Application. John Wiley & Sons, Inc., New York. Vol. 2.

GERSTEIN, G. L., and B. MANDELBROT. 1964. *Biophys. J.* **4**:41.

GLUSS, B. 1967. *Bull. Math. Biophys.* **29**:233.

GRANIT, R., D. KERNELL, and Y. LAMARRE. 1966. *J. Physiol. (London).* **187**:379.

HILL, S., C. E. POLKEY, and T. D. WILLIAMS. 1966. *In* Muscular Afferents and Motor Control. R. Granit, editor. John Wiley & Sons, Inc., New York. 363.

JUNGE, D., and G. P. MOORE, 1966. *Biophys. J.* **6**:413.

KATZ, B., and R. MILEDI. 1963. *J. Physiol. (London).* **168**:389.

MOORE, G. P. 1965. *Electroencephalog. Clin. Neurophysiol.* **18**:531. (Abstr.)

MOORE, G. P., D. H. PERKEL, and J. P. SEGUNDO. 1966. *Ann. Rev. Physiol.* **28**:493.

PAPOULIS, A. 1965. Probability, Random Variables and Stochastic Processes. McGraw-Hill Book Co., Inc., New York.

PERKEL, D. H., G. L. GERSTEIN, and G. P. MOORE. 1967. *Biophys. J.* **7**:391.

SEGUNDO, J. P., D. H. PERKEL, and G. P. MOORE. 1968. In UCLA Forum in Medical Sciences. Number 11. The Interneuron. M. A. B. Brazier, editor. University of California Press, Berkeley and Los Angeles, Calif.

SEGUNDO, J. P., D. H. PERKEL, G. WYMAN, H. HEGSTAD and G. P. MOORE. 1968. *Kybernetik.* **4**:157.

STEIN, R. B. 1965. *Biophys. J.* **5**:173.

STEIN, R. B. 1967. *Biophys. J.* **7**:38.

TAUC, L. 1962. *J. Gen. Physiol.* **45**:1077.

TENHOOPEN, M., and A. A. VERVEEN. 1963. *In* Nerve, Brain and Memory Models. N. Wiener and J. P. Schadé, editors. Elsevier N.V. Uitqevers Mij., Amsterdam-C., 8.

VERVEEN, A. A., and H. E. DERKSEN. 1965. *Kybernetik.* **2**:152.

VERVEEN, A. A., H. E. DERKSEN, and K. L. SCHICK. 1967. *Nature.* **216**:588.